Original Article

Comparative Evaluation of Dicarboxylic Acid Crosslinkers in Tailoring Carboxymethyl Tamarind Gum Hydrogel Films for Wound Healing Applications

Vishwajeet Sampatrao Ghorpade, Remeth Jacky Dias, Akanksha Vidyadhar Gade, Sanjay Ankush Salgar, Sanjay Kumar Banerjee, Kailas Krishnat Mali

DOI: 10.34172/PS.026.43463

To appear in: Pharmaceutical Science (https://pstbzmed.com/)

Received date: 5 Nov 2025

Revised date: 25 Jan 2026

Accepted date: 23 Feb 2026

Please cite this article as: Ghorpade VS, Dias RJ, Gade AV, Salgar SA, Banerjee SK, Mali KK. Comparative evaluation of dicarboxylic acid crosslinkers in tailoring carboxymethyl tamarind gum hydrogel films for wound healing applications. Pharm Sci. 2026. doi: 10.34172/43463

Comparative evaluation of dicarboxylic acid crosslinkers in tailoring carboxymethyl tamarind gum hydrogel films for wound healing applications

Vishwajeet Sampatrao Ghorpade[1] https://orcid.org/0000-0002-7324-3666, Remeth Jacky Dias[2] https://orcid.org/0000-0002-8234-9630, Akanksha Vidyadhar Gade[3] https://orcid.org/0009-0001-1124-1809, Sanjay Ankush Salgar[4] https://orcid.org/0009-0007-2297-2387, Sanjay Kumar Banerjee[4] https://orcid.org/0000-0002-0044-0984, Kailas Krishnat Mali[3] https://orcid.org/0000-0002-1046-9860

[1]Department of Pharmaceutics, Krishna Institute of Pharmacy, Krishna Vishwa Vidyapeeth (Deemed to be University), Karad-415539, Maharashtra, India
[2]Department of Pharmacy, Government College of Pharmacy, Vidyanagar, Karad 415124, Tal-Satara, Maharashtra, India
[3]Department of Pharmaceutics, Adarsh College of Pharmacy, Near MIDC, Khambale (Bha.), Vita Tal- Khanapur 415311 Dist- Sangli, Maharashtra, India
[4]Department of Biotechnology, National institute of Pharmaceutical Education and Research (NIPER), Guwahati 781101 Assam, India

Running Title: Dicarboxylic acid crosslinked CMTG hydrogels

Corresponding author
Dr. Kailas Krishnat MaliDepartment of Pharmaceutics
Adarsh College of Pharmacy,
Near MIDC, Khambale (Bha.),
Vita Tal- Khanapur 415311 Dist- Sangli, Maharashtra, India
Mobile: +91 9271546968, email- malikailas@gmail.com

ABSTRACT

Background: This research introduces a novel comparative study of maleic acid (MA) and succinic acid (SA) as alternative eco-friendly dicarboxylic acid crosslinkers to the frequently utilized citric acid (CA) for carboxymethyl tamarind gum (CMTG) hydrogel films, specifically for wound healing purposes. The study aimed to enhance the mechanical strength and structural integrity of CMTG hydrogel films while maintaining sustained drug release performance, as compared to the conventional CA-crosslinked hydrogel films.

Methods: Hydrogel films were fabricated through an esterification-based crosslinking process using CA, MA, and SA. The resulting films were characterized by ATR-FTIR and thermal analysis, and systematically evaluated for carboxyl content, wettability, tensile strength, porosity, swelling ratio, drug loading and release, protein adsorption, permeability, cytocompatibility, and in vitro wound healing efficacy.

Results: ATR-FTIR and thermal analyses confirmed successful ester crosslink formation. MA-crosslinked hydrogels (HM) exhibited the highest carboxyl content (538.4 ± 5.1 mEq/100 g), contact angle (80.76 ± 2.87°), and tensile strength (95.82 ± 1.47 MPa), along with reduced porosity (45.19 ± 0.22%) compared to CA (HC) and SA (HS) hydrogel films. Crosslinking with MA significantly improved film stability and reduced erosion in phosphate buffer (pH 7.4). Although HM showed lower swelling and drug loading than HC, it achieved sustained moxifloxacin release over 24 h. All hydrogels exhibited minimal protein adsorption, favorable water vapor permeability, effective microbial barrier properties, excellent cytocompatibility, and enhanced in vitro wound closure relative to control.

Conclusion: Maleic acid serves as a promising green crosslinker for developing mechanically robust, biocompatible, and functionally stable CMTG hydrogel films with strong potential for wound healing applications.

Keywords: Carboxymethyl tamarind gum, crosslinking agents, hydrogels, maleic acid, succinic acid.

Introduction

Hydrogels are three-dimensional crosslinked polymeric networks capable of absorbing and retaining substantial amounts of water.[1] Owing to their high water content, biocompatibility, and adjustable mechanical characteristics, they are widely employed in numerous biomedical applications. Moreover, their ability to enable controlled release of drugs and therapeutic agents makes them highly suitable for advanced drug delivery systems.[2–4] Additionally, their high-water content makes them useful for wound healing applications, as they can mimic the natural hydration levels of tissue.[5] Hydrogels can be prepared using natural or synthetic polymers, however natural polymer-based hydrogels have gained popularity amongst the researchers due to their biocompatibility, biodegradability and sustainability [6]. The natural polymer-based hydrogels may present some challenges such as inferior mechanical properties and stability as compared to the synthetic hydrogels, however chemical modification of natural polymers, combination with synthetic polymers and using appropriate crosslinking strategies can enhance their performance.[7–9]

Hydrogels derived from natural polymers can be synthesized through various crosslinking techniques. These include physical crosslinking, which relies on non-covalent

interactions such as hydrogen bonding, ionic attraction, and hydrophobic association, as well as chemical crosslinking, which involves the formation of covalent bonds between polymer chains.[10] Physically crosslinked natural polymer-based hydrogels have a disadvantage of poor mechanical strength, which limits their applicability in areas where robustness is required.[11] On the other hand, chemically crosslinked hydrogels provide excellent mechanical strength, but most of the synthetic crosslinking agents used in their preparation exhibit potential toxicity.[12] This has directed researchers towards nontoxic natural crosslinking agents such as genipin, vanillin, proanthocyanidin, epigallocatechin, and polycarboxylic acids.[13–16] Polycarboxylic acids, including citric acid (CA), tartaric acid, maleic acid, succinic acid, malic acid, and others, have been investigated for their potential as crosslinking agents in the development of natural polymer-based hydrogels.[17–19] These crosslinking agents crosslink the polymer chains through an esterification-crosslinking mechanism.

Tamarind gum (TG), obtained from the endosperm of *Tamarindus indica* seeds, is a natural polymer that exhibits biodegradability, biocompatibility, and noncarcinogenic, nonirritant properties, making it suitable for use in pharmaceutical, cosmetic, and food applications. Despite these benefits, TG has some inherent limitations, such as its unpleasant odor, dull color, and poor solubility in water, which can be addressed through functional derivatization.[20] Carboxymethyl tamarind gum (CMTG) is a chemically modified form of TG with low biodegradability and high swellability, which is utilized in the production of hydrogels due to its gelling properties and ability to modify the release profile of drugs. To date, CMTG-based hydrogels have been prepared by combining it with other natural and synthetic polymers.[21–25] Our team has reported the preparation of hydrogel films (HFs) of CMTG alone for the delivery of model drug (moxifloxacin), using CA as a crosslinking agent.[26] CA has been extensively explored as a crosslinking agent for natural polymer-based hydrogels due to its cost-effectiveness and environmental friendliness, making it an attractive choice for industrial applications.[27] The molecular structure of CA includes three carboxyl groups which allow it to effectively crosslink with natural polymers, enhancing the mechanical properties of the resulting hydrogels.[28] However, we observed that the CMTG HFs exhibited rapid erosion after achieving swelling equilibrium, which may be attributed to the tendency of CMTG to form intrapolymer crosslinks to a greater extent than the interpolymer crosslinks, as observed in the case of carboxymethyl cellulose (CMC).[29]

According to certain research studies, the use of dicarboxylic acids such as maleic acid (MA) and succinic acid (SA) as crosslinking agents has resulted in hydrogels with improved mechanical strength compared to CA due to the formation of a greater number of interpolymer crosslinks.[30,31] Priya and co-workers (2019) reported that fumaric acid crosslinked CMC samples exhibited better thermal stability than CA crosslinked CMC samples, suggesting improved interpolymer crosslinking of CMC with fumaric acid compared to CA.[32] Consequently, there is a need to investigate the effect of such dicarboxylic acids as crosslinking agents on the various properties of CMTG HFs and determine whether they are more efficient in crosslinking CMTG than CA. To date, no studies have investigated the use of dicarboxylic acids, specifically MA or SA, as crosslinking agents for CMTG hydrogels.

This study introduces MA and SA as crosslinkers for CMTG HFs, addressing a gap in prior research that was primarily based on CA for crosslinking. Unlike CA, maleic and succinic acids are dicarboxylic acids that may offer distinct network structures and physicochemical characteristics. The use of MA and SA may enhance rigidity and matrix integrity of the CMTG HFs.[33,34] This novel approach may enable tailored tuning of CMTG hydrogel properties such as swelling and mechanical strength, expanding the functional versatility of CMTG hydrogels beyond CA-crosslinked systems.

In this research, we have evaluated the effects of dicarboxylic acids (MA and SA) on the mechanical properties and matrix integrity of CMTG hydrogels, comparing them to those crosslinked with CA. It also examines how these crosslinkers influence drug loading capacity and release kinetics. Additionally, the study evaluates the biocompatibility and wound healing potential of CMTG hydrogels crosslinked with dicarboxylic acids.

Materials and Methods

Materials

Carboxymethyl tamarind gum powder (average molecular weight: 9.14×10^5 g/mol, degree of substitution: 0.28) was generously provided by Chhaya Industries, Barshi, Maharashtra (India). Analytical-grade citric acid (anhydrous), maleic acid, and succinic acid were obtained from Loba Chemie (Mumbai, Maharashtra, India). Moxifloxacin hydrochloride (MFX) was provided as a gift sample by Chroma Laboratories, Sangareddy, Telangana (India). All other chemicals and solvents used were of analytical grade. A-375 (CRL-1619) cell line was procured from ATCC, Manassas, MD (USA).

Methods

Synthesis of CMTG hydrogel film

CMTG HFs were fabricated following a previously reported procedure with minor modifications.[26] A 2% (w/v) aqueous solution of CMTG was prepared in distilled water using a mechanical stirrer (Remi, Ahmedabad, India). CA, MA and SA were individually added to the polymer solution and stirred for an additional hour. The mixtures were kept side for 2 h to eliminate air bubbles and casted into 9 cm petri plates. Petri plates were dried at 50 °C for 24 h in a hot-air oven and cured at 140 °C for 5 min to promote crosslinking between CMTG and the respective dicarboxylic acids. Subsequently, the films were washed sequentially with distilled water (1 h), isopropyl alcohol, and acetone to remove residual moisture. The resulting HFs were dried and stored in a desiccator until further use. The composition of the films is presented in Table 1.

Table 1. Composition of CMTG hydrogel films

Batch	CMTG (%w/v)	CA (%w/v)*	MA (%w/v)*	SA (%w/v)*	Curing temperature (ºC)	Curing time (min.)
HC	2	20	-	-	140	5
HM	2	-	20	-	140	5
HS	2	-	-	20	140	5

CMTG: Carboxymethyl tamarind gum; CA: Citric acid; MA: Maleic acid; SA: Succinic acid

* indicates % of CMTG concentration.

Total carboxyl content of hydrogel films

Acid-base titration method was used for the determination of the total carboxyl content (TCC) of the HFs.[35–37] A sample of hydrogel films, weighing approximately 100 mg, was dispersed in 20 mL of 0.1N NaOH (devoid of CO_2) and stirred using a magnetic stirrer for 2h. The addition of NaOH disturbed the integrity of the hydrogel film owing to the breakdown of the ester linkage, resulting in dispersion. An excess amount of 0.1N NaOH was then titrated with 0.1N HCl (CO_2 free) using phenolphthalein as an indicator. The total carboxyl content of the hydrogel films was calculated using the following equation:

$$\text{Total carboxyl content (mEq/100g)} = \frac{(V_b - V_a) \times N \times 100}{W} \quad (1)$$

where N represents the normality of HCl (eq/L), V_b is the volume of HCl in the absence of the sample, V_a is the volume of HCl in the presence of the sample, and W is the weight of the sample in grams.

Characterisation of hydrogel films

The infrared spectra of CMTG, CA, MA, SA and HFs were obtained using ATR-FTIR spectrophotometer (Alpha II, Bruker, Tokiyo, Japan). Thermogravimetric analysis (TGA) was carried out on CMTG and HFs by utilizing the Mettler-Toledo TGA/DSC1 thermogravimetric analyzer (Mettler-Toledo, Switzerland).

Wettability of synthesized hydrogels

Manual water contact angle method was used for determination of contact angle of HFs.[38] To perform this technique, a microliter pipette was used to deposit 10 µL of distilled water onto the surface. A digital camera was employed to capture an image of the drop within 5 s. Image J software was used to analyze the images, and the contact angle between the surface and drop was measured. The measurements were performed in triplicate.

Tensile strength of hydrogel films

Texture Analyzer (CT-3/10,000, Brookfield, WI) fitted with a 10 kg load cell was used for the determination of tensile strength of HFs.[39] A film sample measuring 2 × 1 cm was secured between the two clamps of the TA-DGA probe, with a hold time of 60 s. While the lower clamp remained stationary, the upper clamp was moved upward at a speed of 2.0 mm/s over a distance of 6 mm, with a trigger load set at 0.05 N. The force necessary to fracture the hydrogel film was recorded. Each test was conducted in triplicate. The tensile strength at the point of film rupture was calculated using the formula provided below.

$$\text{Tensile strength } (\text{MPa}) = \frac{\text{Force at break (N)}}{\text{Initial cross-sectional area } (\text{mm}^2)} \quad (2)$$

Porosity of hydrogel films

Ethanol replacement method was used for the determination of the porosity of the swollen CMTG HFs.[40] Briefly, hydrogel films equilibrated at pH 7.4 were lyophilized to determine their dry weight (W1). The freeze-dried gels were then immersed in ethanol until saturation, and their weight recorded as W2. Porosity was subsequently calculated using the following equation:

$$Porosity\ (\%) = \frac{W_2 - W_1}{\rho V} \times 100 \quad (3)$$

where V is the volume of the hydrogel film prior to ethanol immersion, and ρ corresponds to the density of ethanol (0.789 g/cm3). All measurements were conducted in triplicate.

Protein adsorption properties of hydrogel films

Lowry method was used for the estimation of protein adsorption capacity of the HFs.[41] The prepared hydrogel films (1 × 1 cm) were immersed in phosphate buffer saline (PBS) containing 200 µg/mL bovine serum albumin (BSA) for 6h at 37 ^{o}C with constant stirring at 100 rpm. Afterwards, the films were rinsed five times with PBS and placed in 5 mL of 1% sodium dodecyl sulfate (SDS) aqueous solution, which was shaken for 1h at 37 ^{o}C using an orbital shaker (Remi, India) to remove the protein adsorbed on the surface of the hydrogel films. The samples were then diluted and analyzed using a UV-visible spectrophotometer (UV1800, Shimadzu, Japan).

To create the calibration curve, a stock solution of BSA (1 mg/mL) was prepared, and different dilutions of BSA (0.05-1 mg/mL) were prepared by mixing the stock solution with PBS in the appropriate proportion. From these dilutions, 0.2 mL was added to test tubes containing 2 mL of alkaline copper sulfate reagent and then incubated at room temperature for 10 min. Subsequently, 0.2 mL of Folin Ciocalteu reagent was added, and the mixture was incubated for 30 min. The absorbance was measured at 660 nm using a UV-visible spectrophotometer. The absorbance values were plotted against the protein concentration to create a calibration curve. Protein adsorption onto the hydrogel films was determined using the absorbance values of the unknown samples and the calibration curve.

Water vapor permeability test

Desiccant method was used for the determination of water vapor transmission rate (WVTR) of the HFs.[42,43] Circular pieces of the hydrogel films, each with a diameter of 1 cm, were cut and then adhered to the mouths of 1 cm-diameter vials containing anhydrous $CaCl_2$. The vials were filled to a level where the distance between the surface of $CaCl_2$ and the lower side of the film was approximately 10 mm. For comparison, reference vials without films were also prepared. These vials, along with those containing the hydrogel films, were placed in desiccators containing a saturated solution of NaCl. The weight of the vials was measured using an analytical balance at specific time intervals, including 0, 6, 24, 36, 48, and 72 h. The weight gain (ΔW) of the vials was recorded during these intervals. The WVTR through the hydrogel films was calculated using the following formula:

$$\mathrm{WVTR} = \frac{\left[(\Delta W/\Delta t) \times 24\right]}{A} \qquad (4)$$

where, (ΔW/Δt) is the slope obtained from the plot of 'w' versus 't', 'W' is the weight gain (g) along the specified time period, 't' (h) and 'A' is the effective transfer area (m^2).

Microbial permeability test

The microbial permeability in the HFs was assessed using a microbial permeability test.[44] In this test, the hydrogel films were secured onto the mouths of 10 mL vials containing 5 mL of nutrient broth. To ensure accuracy, both negative and positive controls were prepared, along with the test samples. The negative control involved sealing a vial containing 5 mL of nutrient broth with a sterilized cotton ball to prevent microbial ingress from the environment. Conversely, the positive control consisted of a vial containing 5 mL of nutrient broth left open to the environment, allowing for potential microbial contamination. All test vials, including the positive and negative controls, were incubated for one week under controlled conditions. After the incubation period, the vials were inspected for any signs of cloudiness or turbidity in the nutrient broth, indicating microbial contamination. A positive result for microbial contamination was recorded if cloudiness or turbidity was observed in the nutrient broth of any vial after the incubation. Conversely, the absence of cloudiness or turbidity indicated that the hydrogel film effectively prevented microbial permeation, thereby demonstrating its barrier properties against microbial ingress.

Swelling study

The method outlined in a previous report was utilized to evaluate the swelling ability of the HFs in water, 0.1 N HCl, and phosphate buffer (pH 7.4).[45] Hydrogel films (1 × 1 cm) were immersed in a specific medium at room temperature, and the swollen films were weighed at specific time intervals for up to 1440 min. The swelling ratio was calculated using the following formula:

$$\text{Swelling ratio (g/g)} = \frac{(W_T - W_0)}{W_0} \quad (5)$$

where W_T is the weight of the swollen hydrogel at time T and W_0 is the weight of the dry hydrogel films. The measurements were performed in triplicate.

Equilibrium wound fluid absorption (EWFA) by the hydrogel films was determined by immersing the pre-weighed hydrogels in a beaker containing 20 mL of simulated wound fluid (SWF, pH=8). The SWF solution consisted of 0.68 g of NaCl, 0.22 g of KCl, 2.5 g of $NaHCO_3$, and 0.35 g of NaH_2PO_4, and was maintained at a temperature of 37°C ± 0.5°C. The swollen hydrogel films were weighed at periodic intervals until they reached equilibrium, and the equilibrium swelling ratio was calculated using following formula: by dividing the weight (in grams) of the swollen hydrogel film at equilibrium by the weight (in grams) of the dry hydrogel film.[46]

$$\text{EWFA (g/g)} = \frac{(W_S - W_D)}{W_D} \quad (6)$$

Where, WS is the weight (g) of the swollen hydrogel film at equilibrium and WD is the weight (g) of the dry hydrogel film.

Drug loading and content

The HFs, weighing approximately 500 mg each, were permitted to absorb an aqueous solution of MFX (10 mg/mL) until equilibrium was achieved. Subsequently, the hydrated HFs were dried in a hot-air oven at 40°C for 24 h. The dried films were cut into small pieces, immersed in 50 mL of distilled water, and stirred using a magnetic stirrer (Remi, India) at 100 rpm for 24 h. The amount of MFX loaded onto the HFs was determined spectrophotometrically (UV-1800, Shimadzu, Japan) at a wavelength of 289 nm, using following formula:

$$\text{Drug loading (mg/g)} = \frac{Amount\ of\ MFX\ (mg)}{Weight\ of\ hydrogel\ film\ (mg)} \times 1000 \quad (7)$$

In vitro drug release

The drug release study was performed by placing an MFX-loaded HF (50 mg) in 10 mL of phosphate buffer solution (pH 7.4) at 37°C. The pH of 7.4 was chosen to simulate physiological conditions, as it closely matches the pH of human extracellular fluids, including blood plasma and interstitial fluid. This helps to evaluate the hydrogel swelling behavior and drug release kinetics under conditions that mimic the wound environment and systemic circulation. At predetermined intervals, 1 mL aliquots of the release medium were withdrawn, diluted appropriately, and subjected to spectrophotometric analysis at 289 nm. The sink conditions were maintained throughout the study. The experiment was repeated thrice to ensure the accuracy and reliability of the results. The drug release data were analyzed using zero-order, first-order, Higuchi, Hixson-Crowell, and Korsmeyer-Peppas kinetic models to elucidate the release mechanism from the HFs.[47–49] The kinetic models were represented as follows:

Zero order model:

$$Q_t = k_0 t + Q_0 \quad (8)$$

First order model:

$$Q_t = Q_0 e^{k_f t} \quad (9)$$

Higuchi order:

$$Q_t = k_h t^{0.5} \quad (10)$$

Hixon-Crowell model:

$$Q_0^{1/3} - Q_0^{1/3} = k_s t \quad (11)$$

Korsmeyer–Peppas model:

$$Q_t/Q_\infty = kt^n \quad (12)$$

where, Q_t signifies the total percentage of the drug released at a specific time t, whereas Q_0 indicates the initial drug quantity. The constants for the release rate are denoted as k_0, k_f, k_h, k_s, and k, corresponding to the zero-order, first-order, Higuchi, Hixon-Crowell, and Korsmeyer-Peppas models, respectively. The 'n' parameter is the diffusion coefficient, which depends on the interaction between the drug and the hydrogel matrix components.

Cytotoxicity study

Cytotoxicity of HFs was assessed in A-375 human melanoma cells using the MTT assay. Cells were seeded at 2×10^4 cells/well in 96-well plates with DMEM containing 10% FBS and antibiotics and incubated at 37 °C, 5% CO_2. HFs (2 cm^2/mL) were pre-soaked in serum-free DMEM for 24 h, and the extract was collected, pH-adjusted (7.0–7.4), and diluted 16-fold (6.25% v/v). Confluent cells (~80%) were treated with 100 µL of the extract for 24 h. DMEM alone served as control. After treatment, 100 µL of 0.5 mg/mL MTT was added, incubated for 4 h in the dark, followed by dissolution of formazan crystals in 100 µL DMSO. Absorbance was measured at 570 nm (reference 630 nm) using an Epoch microplate reader (BioTek, USA).

Scratch wound assay

Wound-healing potential of CMTG HFs was assessed in A-375 cells via a scratch assay. Confluent monolayers were scratched with a pipette tip, washed with PBS, and treated with 6.25% v/v hydrogel extract, while untreated wells served as controls. Wound closure was imaged at 0, 4, 8, 12, and 24 h under a phase-contrast microscope, and percentage closure was quantified using ImageJ software.

Statistical analysis

Data were analyzed using one-way ANOVA followed by Tukey's multiple comparison test. Differences were considered statistically significant at $p < 0.05$.

Results and Discussion

Synthesis of CMTG hydrogel film

CMTG HFs were produced through mechanisms primarily involving esterification-crosslinking (See Figure 1). At high temperatures, CA forms anhydride, which is highly reactive. When this anhydride reacts with the hydroxyl group of CMTG, it liberates a carboxyl group,

which then becomes available to form another anhydride, and potentially undergoes further esterification and crosslinking with another CMTG molecule. This reaction is typically carried out under semi-dry conditions to promote anhydride formation and facilitate efficient reactions at high temperatures.[50]

In the case of MA and SA, the mechanism of crosslinking via the two cyclic anhydride intermediates cannot be adopted for the interpretation of the crosslinking stage because these compounds contain only two carboxylic groups. When heated, MA forms a cyclic anhydride, followed by the formation of ester crosslinks with the hydroxyl group of CMTG.[51] The actual mechanism underlying the formation of ester crosslinks in case of MA in absence of sodium hypophosphite (catalyst) is still unknown. On the other hand, there are two routes for crosslinking with SA: direct esterification (primary) and ionization. In direct esterification, both carboxylic groups of SA may form ester crosslinks with the two hydroxyl groups of different CMTG chains. In ionization, a cation exchange takes place between the sodium salt of CMTG and the carboxylic group of SA.[52]

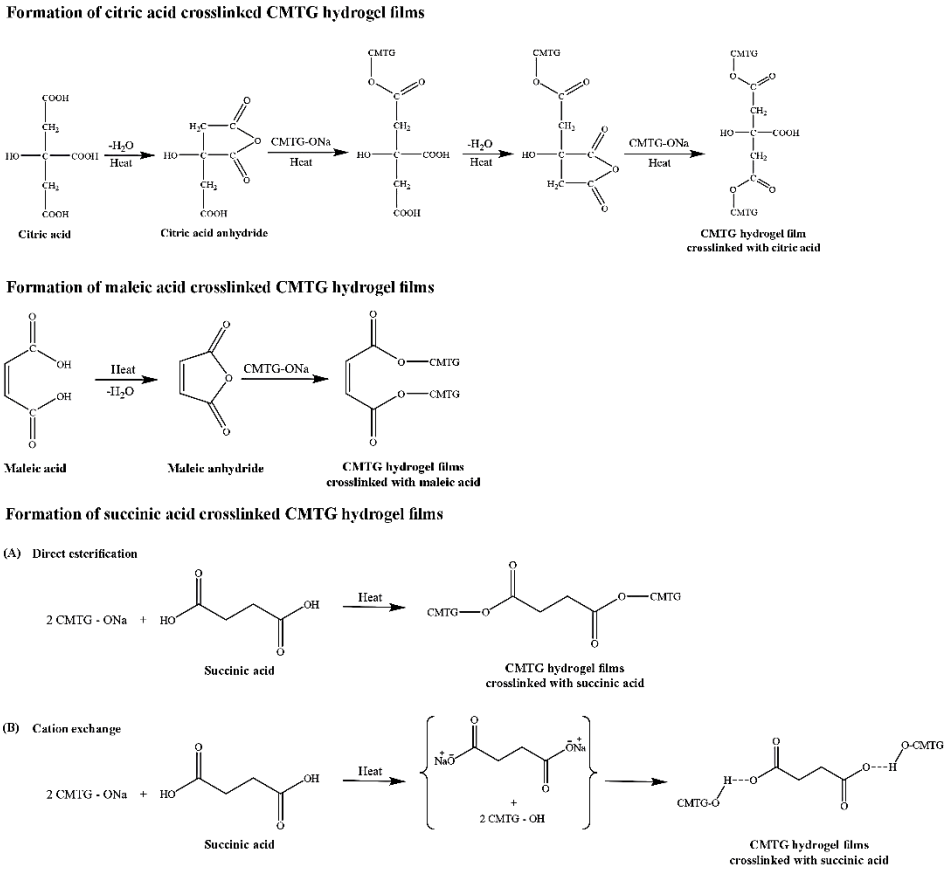

Figure 1. Possible crosslinking reactions of CA, MA, and SA with CMTG.

To obtain films with better integrity and optimal swellability, a curing temperature of 140^{o}C and curing time of 5 min were found to be essential. Although CMTG HFs can be produced at temperatures below 140 °C, longer curing times are required. However, a curing time of 5 min was considered appropriate to expedite production. Photographs of the CA-, MA-, and SA-crosslinked films are shown in Figure 2.

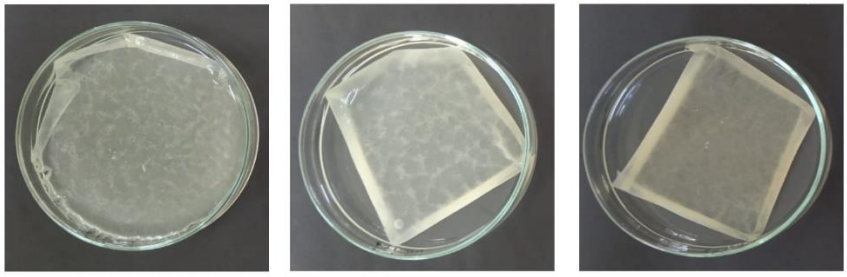

Figure 2. CA, MA and SA crosslinked films of CMTG

Thickness of hydrogel film

The thicknesses of the CMTG HFs were measured using a micrometer screw gauge. The thicknesses of the HFs are presented in Table 2. According to the results, HM demonstrated the maximum thickness, followed by HC and HS. This can be attributed to the maximum crosslinking interactions observed in the case of MA, followed by those of CA and SA. An increase in crosslinking can lead to the binding of more polymer chains, resulting in an increase in the density of the HFs and, subsequently, the thickness.[53]

Table 2. Thickness, total carboxyl content, contact angle, tensile strength and porosity of hydrogel films.

Batch	**Thickness (µm)**	**Total carboxyl content (mEq/100g)**	**Contact angle (°)**	**Tensile strength (MPa)**	**Porosity (%)**
HC	563.33±5.16	501.3±5.2	64.21±2.19	83.99±2.35	58.72±0.15
HM	566.66±5.22	538.4±5.1	80.76±2.87	95.82±1.47	45.19±0.22
HS	556.66±5.13	409.2±6.3	73.13±2.63	49.91±0.78	67.05±0.18

Total carboxyl content of hydrogel films

The carboxyl group content in crosslinked HFs is directly related to the degree of crosslinking, and can have a significant impact on the properties of the hydrogel films. The effects of CA, MA, and SA on TCC of the HFs are presented in Table 2. The TCC of HM was found to be significantly greater than that of HC and HS ($p < 0.001$). This suggests that the incorporation of MA as a crosslinking agent resulted in the formation of a maximum number of crosslinks in the CMTG HF compared to CA and SA. Although the concentration of CA and MA was the same (i.e., 20% of CMTG), the MA-crosslinked HF exhibited the highest TCC, likely due to the higher molar concentration of MA than that of CA. As a result, more MA molecules were involved in the crosslinking reaction than CA molecules. Conversely, the TCC values of the SA-crosslinked CMTG HF were lower than those of the MA- and CA-crosslinked films, despite having a molecular weight similar to that of MA. This can be attributed to the cis-orientation of carboxyl groups in MA, which makes it more reactive towards esterification than SA.[54]

ATR-FTIR spectroscopy

Figure 3A shows the ATR-FTIR spectra of CMTG and CMTG HFs. The spectrum of CMTG exhibits characteristic bands at 3259 cm^{-1} (OH stretching), 2906.97 cm^{-1} (asymmetric -CH stretching), 1744 cm^{-1} (C=O stretching), 1582 cm^{-1} and 1409 cm^{-1} (-COO-), and 1015 cm^{-1} (C-O-C stretch of glycosidic linkage). The spectra of the CMTG HFs exhibited the presence of all the characteristic peaks associated with CMTG as well as the emergence of an additional peak at 1724 cm^{-1}, which corresponds to the carbonyl bond of the ester crosslinks. The intensity of the carbonyl peak was higher in the case of HM than in HC, while the intensity of the carbonyl peak in HS was lower than that of HC (see Figure 3B). This suggests that MA-crosslinked CMTG HFs exhibited a greater extent of ester crosslinks, whereas SA-crosslinked HFs exhibited fewer ester crosslinks than CA-crosslinked HFs. The reduced number of ester crosslinks in succinic acid SA-crosslinked HFs, as compared to CA-crosslinked HFs, can be attributed to the lower reactivity of SA in esterification reactions relative to CA. CA possesses three carboxyl groups, in contrast to the two carboxyl groups of SA, thereby offering more reactive sites for esterification.[55]

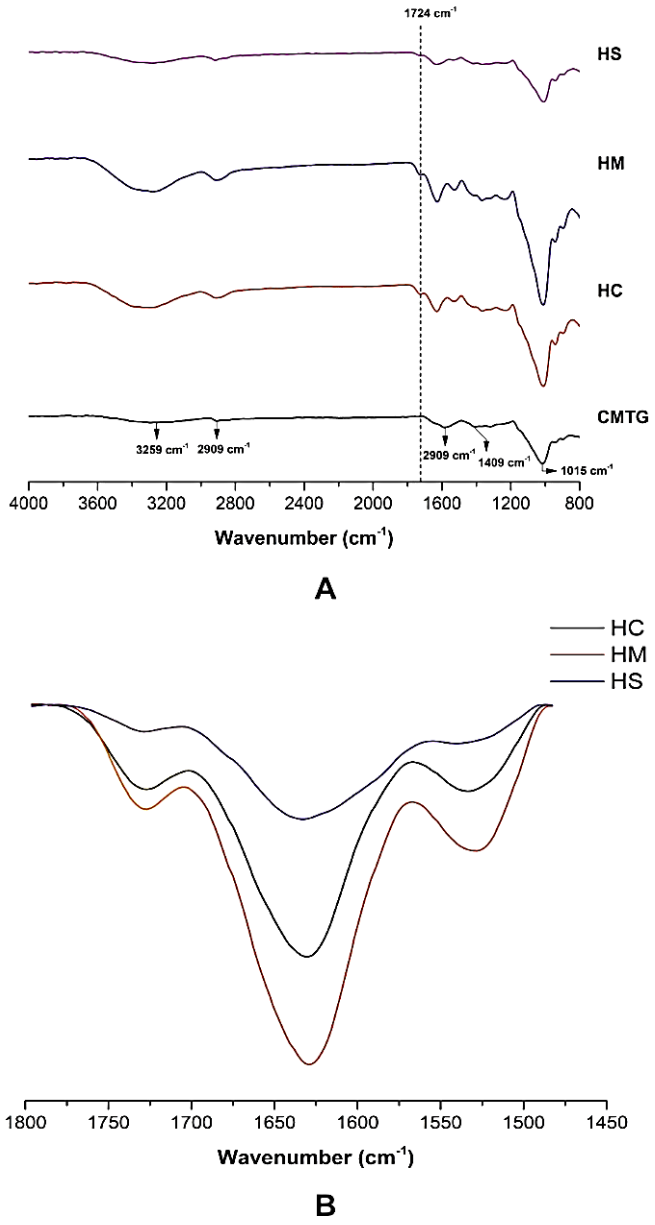

Figure 3. ATR-FTIR spectra of CMTG and hydrogel films (A) and intensities of ester carbonyl peaks of hydrogel films (B) crosslinked using CA, MA and SA.

Thermal analysis

Figure 4 presents the TGA and DTG thermograms of CMTG and the hydrogel films (HFs). Both samples exhibited three distinct stages of thermal decomposition. In the TGA profile of CMTG, the first weight loss of approximately 12.1% occurred between 30–200°C, corresponding to the evaporation of free and bound water. The second stage, observed between 200–400°C, showed a major weight loss of 50.61%, attributed to the degradation of glycosidic linkages within the polymer backbone. The final stage, occurring between 400–600°C with a 14.08% weight loss, represents the complete thermal decomposition and

combustion of the polymer matrix.[56,57] The maximum degradation temperature (T_m) as determined by DTG for CMTG was found to be 299.93°C.

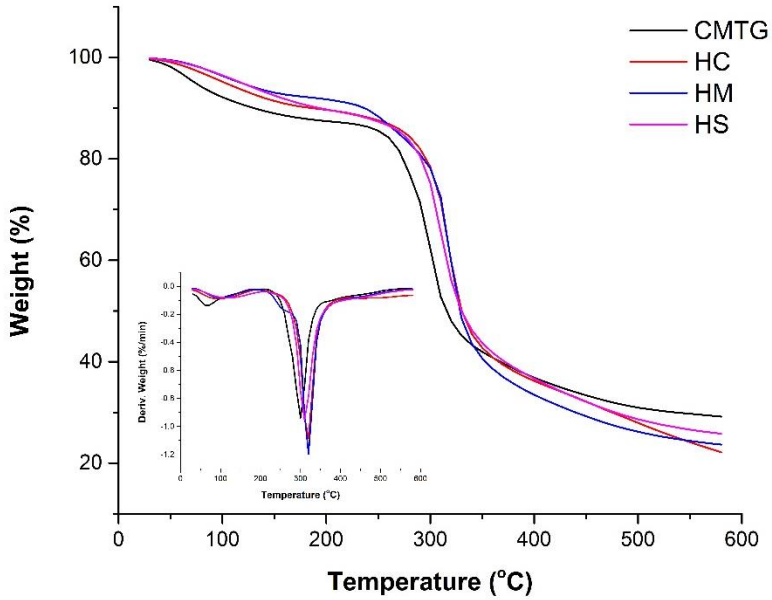

Figure 4. TGA and DTG thermograms of CMTG and hydrogel films

HC, HM, and HS exhibited a reduced weight loss in the first degradation stage, which can be attributed to the formation of covalent bonds between polymer chains during crosslinking. This crosslinked network likely restricted the mobility of polymer chains and limited the hydration of the hydrogel matrix. The enhanced thermal stability of the hydrogel films (HFs) was further confirmed by the observed increase in their decomposition temperatures (T_m values: HC – 320.19 °C, HM – 319.79 °C, and HS – 310.06 °C). This shift in Tm indicates that crosslinking effectively improved the thermal resistance of the HFs. The final degradation stage of the HFs showed a higher weight loss compared to CMTG, which may be due to the breakdown of additional crosslinked structures formed during hydrogel synthesis. This phenomenon can be attributed to the thermal cleavage of ester bonds within the HFs at elevated temperatures. Such a process may produce volatile degradation products, thereby contributing to a greater weight loss than that observed in the pure polymer.The ATR-FTIR analysis results showed that the MA-crosslinked HFs exhibited a greater extent of crosslinking compared to the CA-crosslinked films. However, the DTG curve revealed similar T_m values for HC and HM. This may be ascribed to the presence of grafted CA in HC, where only one COOH of CA esterifies the hydroxyl group of CMTG, and the other two COOH groups are free or in anhydride form, may lead to the formation of new crosslinks in HC during the TGA process

when the temperature exceeds 140°C. This is because the free COOH groups or those in anhydride form of such grafted CA may esterify hydroxyl groups on neighboring CMTG chains.

The findings of the ATR-FTIR and TGA analyses were consistent with the results of the TCC of the CMTG HFs.

Wettability of hydrogel films

The wetting behavior of the plain CMTG film and CMTG HFs was evaluated by measuring the static contact angle of a water droplet on their surface at five different locations. The mean of the contact angles was taken as the static contact angle. A lower contact angle (less than 65^{o}) indicates better wetting and a more hydrophilic surface, while a higher contact angle (more than 65^{o}) suggests poor wetting and a more hydrophobic surface.[58] Table 2 displays the contact angles of the HFs. The contact angles were ranked in the following order: CMTG < HC < HS < HM. The hydroxyl groups of CMTG become involved in ester formation due to crosslinking, which reduces its hydrophilicity. The surfaces of the CMTG and CA-crosslinked films were found to be hydrophilic, while the surfaces of the SA and MA-crosslinked films were hydrophobic. HM showed a more hydrophobic surface than the other films due to a greater extent of crosslinking. It was noteworthy that HC showed a hydrophilic surface despite having more crosslinks than HS. This may be attributed to the presence of free COOH and hydroxyl groups of the CA crosslinks, which may impart hydrophilicity to the surface of the CA-crosslinked HFs.

Tensile strength and porosity of hydrogel films

The tensile strength and porosity of the CMTG HFs is depicted in Table 2. The tensile strength values found in the range of ~ 50-96 MPa, are characteristic of dry-state hydrogel films, which are structurally more robust due to reduced polymer swelling and stronger intermolecular interactions. These values indicate a baseline robustness suitable for practical handling and application before hydration. Similar values related to the tensile strength have been reported in case of PVA-CMC-NaAlg hydrogel films meant for open wound management.[59] In contrast, hydrated hydrogels typically exhibit significantly lower tensile strength, as water acts as a plasticizer, increasing chain mobility and flexibility . The determination of tensile strength offers valuable information regarding the mechanical strength of a film. The results indicate that the tensile strength of HM is significantly higher than that of HC and HS ($p<0.05$). This finding supports our contention that MA-crosslinked HFs

exhibit a greater degree of crosslinking than CA-crosslinked HFs and SA-crosslinked HFs. HS exhibited lowest tensile strength.

The high porosity of HFs facilitates the absorption of wound exudates and the exchange of gases, thereby expediting the wound healing process. HS demonstrated significantly greater porosity compared to HC and HM ($p<0.05$). The porosity of HM was observed to be lower, further confirming a greater degree of crosslinking in HM than in HC and HS.

Protein adsorption properties of hydrogel films

The connection between a wound dressing's ability to bind proteins and its potential to promote cell adhesion is well-established. In this study, Bovine Serum Albumin (BSA), which is the most prevalent protein in blood, was selected as the model protein to evaluate the protein adsorption behavior of HFs. The protein adsorption properties of organic acid crosslinked CMTG HFs are summarized in Table 3. These results indicate that all films exhibit minimal protein adsorption, which is advantageous for their potential application as hydrogel wound dressings.[60,61] These dressings typically require a low amount of protein adsorption to fulfill their intended functions in facilitating wound healing processes. When comparing the films, HC showed less protein adsorption than HM and HS, which can be attributed to its hydrophilic nature. As hydrophobicity of the films increased in the case of HS and HM, protein adsorption also increased.

Table 3. Protein adsorption, permeability properties, equilibrium swelling ratio (ESR), equilibrium wound fluid absorption (EWFA) and drug loading of CMTG hydrogel films

Batch	Protein adsorption (mg/cm^2)	WVTR (g/m^2)	Microbial permeability	ESR (g/g)	EWFA (g/g)	Drug loading (mg/g)
HC	0.124	1177.1	-ve	18.73±0.75	16.38±0.38	302.91±1.24
HM	0.155	998.4	-ve	8.75±0.24	9.23±0.52	191.45±1.98
HS	0.141	1424.2	-ve	16.12±0.69	12.05±0.27	231.02±1.55

WVTR: Water vapour transmission rate

Permeability properties

Optimal water vapor permeability of HF is the key factor for wound healing. It prevents moisture buildup that can cause maceration and delayed healing while avoiding excessive water loss that leads to desiccation and impaired recovery.[62–64] Proper permeability maintains

a balanced wound environment, aiding cell migration, proliferation, and angiogenesis, and regulates temperature and pH for tissue repair.[65,66] Furthermore, it ensures patient comfort by providing a breathable, non-occlusive environment, enhancing adherence to wound care and patient satisfaction.

The results of water vapor transmission rate (WVTR) of CMTG HFs are presented in Table 3. The WVTR value for the control vial (open vial) was determined to be 2545.45 g/m^2. The vials coated with HFs demonstrated a significantly lower water vapor transmission rate than the uncovered vials. There are no specific minimum requirements or optimal values for WVTR according to the epic3 guidelines, as long as the dressing is genuinely "semi-permeable" and requires changing when moisture accumulates under the dressing.[67] Consequently, it can be concluded that the CMTG HFs prepared in this study can effectively transmit water vapor as they were designed to be changed every 24 h. HS demonstrated higher WVTR due to poor crosslinking, while the HM showed the lowest WVTR due to greater crosslinking.

Wounds create an environment favorable for microbial colonization and growth due to their warmth, moisture, and nutrient availability, which can hinder healing.[68,69] External infections worsen this by further delaying healing. In order to effectively prevent pathogens from entering wounds, it is essential for dressings to provide adequate protection for the wound surface. The microbial permeability test was implemented to assess the efficacy of CMTG HFs in acting as a barrier against pathogens, as shown in Table 3.

Initially, on day 0, no microbial growth was observed in any of the vials containing the nutrient broth with the HFs, the negative control, or the positive control. However, by the 7th day, microbial growth was evident in both the negative and positive control groups, while the vials sealed with the HFs remained free from microbial growth. This suggests that all the HFs effectively prevented microbial permeation in an open environment.

Swelling study

The influence of CA, MA and SA as crosslinkers on the swellability of HFs was investigated in phosphate buffer at pH 7.4. Figure 5 illustrates the swelling behavior of the HFs, and the equilibrium swelling ratios (ESR) of the HFs are provided in Table 3.

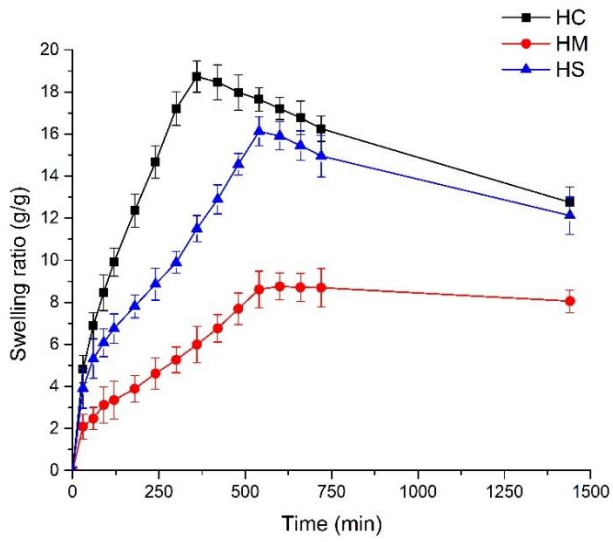

Figure 5. Swelling behavior of CMTG hydrogel films in phosphate buffer (pH 7.4).

The time required for HC, HM, and HS to reach equilibrium was found to differ. While HC achieved equilibrium after 360 min, HM and HS required 600 min and 540 min, respectively. Additionally, HC exhibited the highest ESR ($p<0.05$), followed by HS and then HM. The swellability of hydrogels is generally influenced by the extent of crosslinking.[70,71] In comparison to HS, HC achieved swelling equilibrium at a faster rate and exhibited a higher ESR value, although the former displaying a greater degree of crosslinking. This may be attributed to higher hydrophilicity of HC compared to HS, as well as the electrostatic repulsion between adjacent carboxylate ions (COO^-) resulting from the ionization of free carboxylic acid groups of CA crosslinks and between carboxylate ions of CA crosslinks and ionized carboxyl groups of CMTG at pH 7.4.[52,72] MA and SA lack free COOH groups in their crosslinks. On the other hand, HM required a longer time to reach equilibrium compared to HC and HS, and displayed the lowest ESR. This may be attributed to the increased degree of crosslinking, which resulted in reduced porosity and a hydrophobic nature of HM.

Despite exhibiting superior swellability compared to HM, HC and HS displayed rapid erosion after achieving equilibrium. This can be attributed to the lower crosslinking density in HC and HS compared to HM. HFs for wound healing are designed to maintain their structural integrity over time, resisting rapid erosion to ensure sustained therapeutic effects and protection of the wound site. Rapid erosion of HFs could compromise their function, leading to inadequate drug delivery, loss of moisture regulation, and insufficient barrier against microbial invasion.[46,73] This makes CA and SA-crosslinked CMTG HFs less efficient as a wound healing biomaterial. Although most of the researchers, including ourselves, have successfully

used CA as a crosslinker for the development of hydrogels based on carboxymethylated polymers, due to the issue of rapid erosion at pH 7.4, we had to combine other water-soluble polymers with carboxymethylated polymers so as to enhance interpolymer crosslinks rather than formation of intra-polymer crosslinks and minimize the rate of erosion.[50,74–78] The MA-crosslinked CMTG HFs exhibited greater resistance to erosion; however, poor swellability was a notable drawback.

The equilibrium swelling of HFs in simulated wound fluid was investigated to assess their appropriateness as wound dressings (see Table 3). The findings of the equilibrium wound fluid absorption were consistent with the ESR observed in the hydrogels. HC demonstrated high wound fluid absorption, whereas HM exhibited low wound fluid absorption. Although higher absorption of wound fluid (exudate) is generally advantageous, excessive swelling can compromise the structural integrity of HFs.[79] Consequently, the HM hydrogels, with their lower EWFA (9.23 g/g) and enhanced mechanical strength, may provide a more suitable balance for certain wound types that require reduced fluid absorption and increased structural support.

MFX loading and release

The diffusion process was employed to load moxifloxacin hydrochloride (MFX) into crosslinked HFs, and the results of drug loading are presented in Table 3. We selected MFX because it is a broad-spectrum fluoroquinolone antibiotic widely used to treat bacterial infections, including those in wounds, due to its effectiveness against a wide range of Gram-positive and Gram-negative bacteria.[80] Additionally, physicochemical properties of MFX, such as water solubility and stability, make it suitable for incorporation into hydrogel films for sustained drug delivery. It was observed that the drug loading in all hydrogel batches primarily depended on their swellability and hence on their extent of crosslinking. An increase in crosslinking density generally results in a decrease in the drug loading capacity of hydrogels. This is due to the tighter network structure that forms as crosslinking density increases, which can limit the space available for drug molecules to be encapsulated within the hydrogel matrix.[81,82] The other factors responsible for holding the MFX within the hydrogel matrix can be electrostatic interaction and hydrogen bonding between MFX and hydrogel components. In distilled water (pH 6.2), piperazinyl group of MFX has a positive charge, while the free COOH groups in HFs can undergo partial ionization to form carboxylate ions.[83,84] These carboxylate ions can potentially interact with the positively charged piperazinyl group of MFX, facilitating

binding or association.[85] The presence of hydrogen bonding between MFX and components of CMTG HFs was confirmed from ATR-FTIR analysis of pure MFX and MFX loaded HFs (see Figure 6). MFX showed characteristic peaks at 3524 cm-1 (O-H str; COOH), 3470 cm^{-1} (N-H str), 2521 cm^{-1} (NH_2^+ str) 1704 cm^{-1} (C=O str; COOH), 1618 and 1518 cm^{-1} (C=O str; phenyl breathing), 1451 cm^{-1} (skeletal vibrations of benzene ring), 1175 cm^{-1} (C-O str) and, 1315 and 1357 cm^{-1} (C-F str). Most of the characteristic peaks of MFX were found to be masked by the peaks of hydrogel components, except the peaks representing NH_2^+ stretching and C-O stretching. The intensity of peak associated with NH_2^+ stretching was found to be reduced to a greater extent, whereas peak corresponding to C-O stretching shifted to lower frequency at around 1140 cm^{-1}. This reveals the presence of hydrogen bonding interaction in between MFX and polymer.[86–89]

The order of drug loading was found to be HC>HS>HM. A significant difference was found in the drug loading capacity of all three HFs ($p<0.05$). The high drug loading in HC may be attributed to its high swellability and the electrostatic interaction between MFX and carboxylate ions in HC. Free COOH groups can arise from CA, MA, and SA molecules that esterified OH groups on one chain of CMTG but were unable to esterify OH groups on the other CMTG chain. Under these conditions, these crosslinking agents remain grafted to the polymer chains in the hydrogel, with unreacted (free) COOH groups. According to the results, HM exhibited superior crosslinking compared to HC and HS, and the TCC of HS was lower than that of HM and HC. Therefore, it is less likely that there is a significant quantity of grafted crosslinking agents in the HM and HS samples than HC. It is important to acknowledge that, in addition to the grafted CA, free COOH groups are also present on the CA crosslinks in CA-crosslinked HFs. This may result in maximum drug retention within the hydrogel matrix through electrostatic interaction in HC as compared to HM and HS. It was observed that HM exhibited less MFX loading than HS due to its lower swellability and probably fewer free COOH groups as compared to HS.

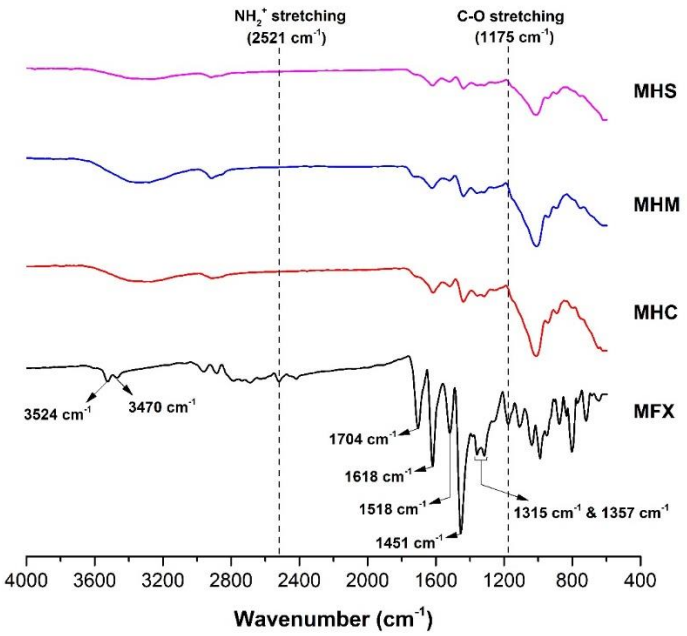

Figure 6. ATR-FTIR spectra of MFX, MFX loaded HC (MHC), MFX loaded HM (MHM) and MFX loaded HS (MHS) hydrogel films.

The MFX release profile from CMTG HFs is presented in Figure 7. All films sustained MFX release for up to 24 h, with an initial burst of 19–25% within the first hour, likely due to surface-associated drug. During drying of the drug-loaded hydrogels, free drug molecules migrate from the bulk to the surface along with solvent, resulting in rapid release upon contact with the dissolution medium.[90]

After 24 h, HC, HM, and HS released 83.52%, 98.94%, and 96.24% of the drug, respectively. The release of MFX was found to be significantly retarded in HC compared to the other HFs despite of high swellability. This could be attributed to three factors. First, extent of crosslinking in HC was less than HM. A low crosslinking density results in longer polymer chains between crosslinks. These chains form physically entangled loops, reducing the mesh size and thereby hindering drug diffusion from the hydrogel matrix.[91] Second, the high swellability of HC can extend the diffusion path of drug molecules, thereby slowing drug release. Third, HC exhibited a greater extent of electrostatic interactions between MFX and carboxylate ions compared to HM and HS, as discussed earlier. Despite high erosion rate of HC, these electrostatic interactions were capable of controlling the release of drug.[92,93] On the other hand, release rate of MFX was higher in HS, possibly due to weaker electrostatic interactions between MFX and carboxylate ions in HS. The sustained drug release profile was observed between 360 and 600 minutes, despite the occurrence of erosion, which can be attributed to

the structural stability and release dynamics of the crosslinked hydrogel matrix. Crosslinked hydrogels are recognized for exhibiting more controlled and sustained release behavior compared to their non-crosslinked counterparts, owing to the formation of a stable, three-dimensional polymeric network. This network preserves its integrity even during gradual erosion, thereby facilitating continued and consistent drug diffusion.[94,95]

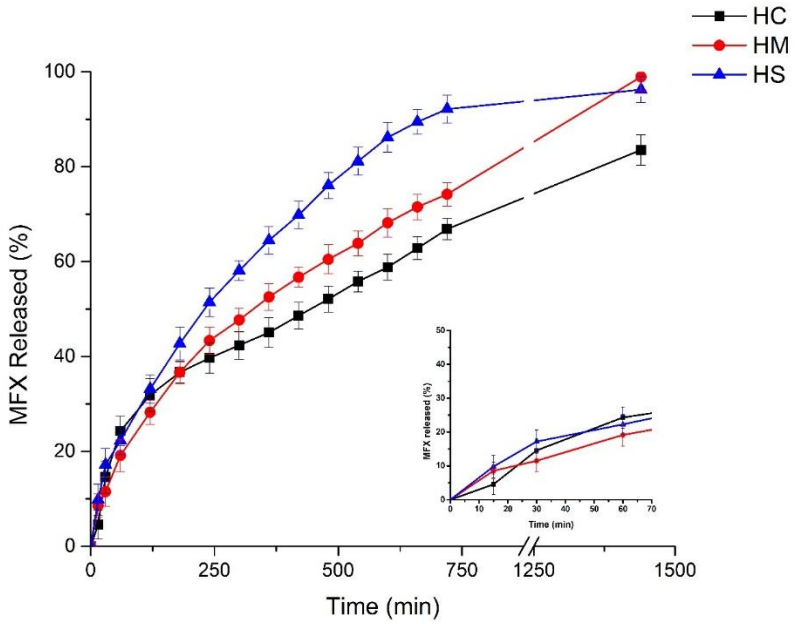

Figure 7. MFX release from CMTG hydrogel films in phosphate buffer (pH 7.4)

Moreover, the drug release mechanism in the CMTG HFs followed non-Fickian (anomalous) diffusion pattern, wherein drug release is governed by a combination of diffusion, polymer relaxation, and matrix erosion. This integrated mechanism enables a smooth and uninterrupted release curve, even as portions of the polymer matrix begin to erode.[96] Consequently, the erosion contributes to the release process without disrupting it, as the core structure of the hydrogel continues to support drug diffusion. HM demonstrated nearly complete drug release while maintaining its matrix integrity, which was a favorable characteristic for a wound healing biomaterial. However, there is a need to enhance its drug loading capacity which can be achieved by increasing its swellability.

The results of release kinetics are presented in Table 4. The release of MFX from all hydrogel batches followed Korsmeyer-Peppas and demonstrated Non-Fickian release behavior, indicating that drug release was governed by mixture of diffusion and polymer chain relaxation.[97]

Table 4: Release kinetics of CMTG hydrogel films.

Batch	Zero order		First order		Higuchi		Hixon-Crowell		Korsmeyer-Peppas		
	K	R^2	K	R^2	K	R^2	K	R^2	K	R^2	n
HC	0.0517	0.8491	0.0014	0.5093	2.4853	0.8248	0.0015	0.6399	1.5111	0.9097	0.577
HM	0.0647	0.8786	0.0015	0.6259	2.6321	0.9891	0.0017	0.7188	1.9050	0.9951	0.586
HS	0.0670	0.7298	0.0014	0.5633	3.1938	0.9199	0.0016	0.6279	2.5579	0.9800	0.573

Cell viability after hydrogel film exposure by MTT assay

A-375 human malignant melanoma cells were chosen for the MTT assay to evaluate cytotoxicity because they are a well-characterized and reproducible *in vitro* model for estimation of cell viability in response to biomaterials. After 24 h HFs extract treatment to A-375 cells, MTT assay was performed to assess the cell viability. The result showed non-significant reduction in cell viability (see Figure 8). A-375 cells were treated with 6.25% v/v (16 times dilution) concentration of HF, and percentage of viable cell recorded after 24 h. The cell viability assay evidenced that HFs were not cytotoxic to A-375 human malignant melanoma cells as there was insignificant difference between readings of control and the HFs.

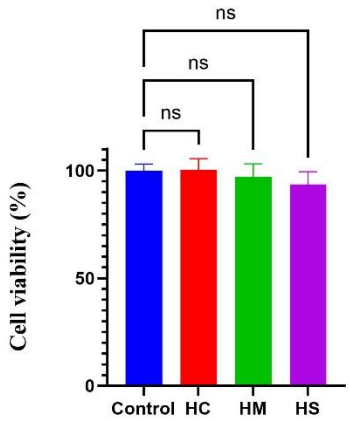

Figure 8. The A-375 cell viability was observed after hydrogel film exposure. Data are expressed as means ±SD (n=5) *p<0.05, ns: not significant vs control.

Wound healing scratch assay

To check the effect of blank CMTG HFs on the cell migration and cell proliferation of A-375 human malignant melanoma cells, a time dependent (0-24 hours) wound scratch assay was performed. A-375 cells form continuous monolayers suitable for creating consistent wounds or gaps by mechanical scratching. Their inherent growth and migration properties make them an effective model to monitor *in vitro* wound closure dynamics. After 24 h of HF treatment, the wound was completely closed compared with only DMEM treated cells. The result shows that the CMTG HF treated cells migrated significantly compared to only DMEM

treated cells. This reveals the potential of blank CMTG HFs to stimulate cell proliferation and migration. This can be possibly due to hydrophilic and biocompatible nature of CMTG, and presence of free COOH groups within the hydrogel matrix. It has been reported that presence of carboxylic acid side groups on the biomaterials promotes cell adhesion and proliferation.[98] HS took more time for wound closure possibly due to a smaller number of free COOH groups than HC and HM.

Although the mechanical strength and post-swelling equilibrium matrix integrity of MA-crosslinked CMTG HFs were better than those of CA-crosslinked HFs, the swellability and drug loading were found to be lower. To overcome this issue, it is proposed that CMTG be combined with polymers like PVA having reactive OH groups, which could improve the hydrophilicity of MA-crosslinked HFs.[75,76] Nascimento and co-workers (2020) discovered that combining CA and SA resulted in enhanced water uptake by PVA films compared to using the crosslinking agents separately.[99] Hence, combining CA and MA in a specific ratio might lead to improved swellability and drug loading for CMTG HFs.

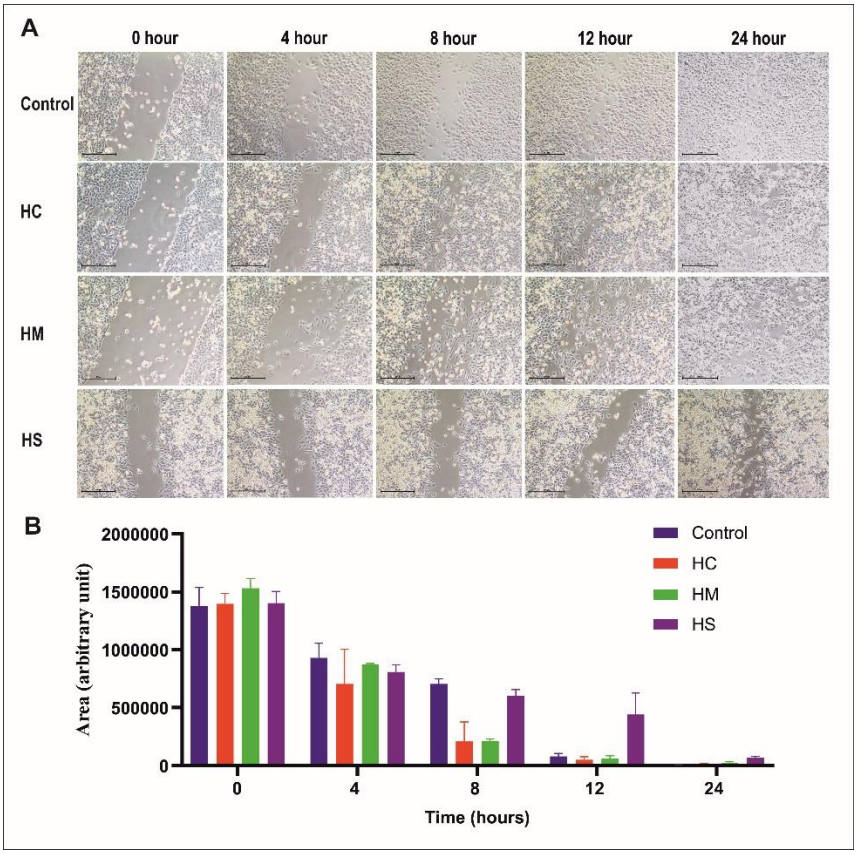

Figure 9. Hydrogel film stimulates cell proliferation and migration in A-375 human malignant melanoma cells. (A) The above images represent the monolayer scratch area with a p200 micropipette tip at different time points (0h to 24 h) after different hydrogel treatments. (B)

The bar graph shows the area of the wound. Wound closure was expressed via a scratch assay of the cells.

Conclusion

This work demonstrates the successful use of MA and SA as dicarboxylic acid crosslinkers for CMTG hydrogels for the first time, offering enhanced mechanical properties compared to conventional CA-crosslinked CMTG HFs. CMTG HFs were prepared by esterification-crosslinking using CA, MA, and SA as crosslinking agents. The maleic acid-crosslinked hydrogel films exhibited better crosslinking of CMTG polymer chains than CA, as confirmed by total carboxyl content, ATR-FTIR, and thermal analysis. MA enhanced the mechanical strength of the HFs and maintained the matrix integrity by minimizing erosion in phosphate buffer (pH 7.4), but it showed lower wettability, porosity, swellability, wound fluid absorption and drug loading than CA and SA crosslinked HFs. Both MA and SA crosslinked HFs were capable of controlling drug release up to 24 h, but the release rate was higher than that of CA crosslinked HFs. The study clearly demonstrated that drug loading and release were closely linked to both the swellability and integrity of the matrix. Greater swellability facilitated increased drug incorporation, while maintaining matrix integrity contributed to the controlled release of the drug. Although the protein adsorption of MA and SA crosslinked HFs was high, it was deemed acceptable for a biomaterial used in wound healing. The films exhibited better water vapor permeability and acted as an efficient barrier against microorganisms. The MTT assay and Scratch test results indicated that the prepared CMTG hydrogel films were cytocompatible and supported cell proliferation and migration.

The overall study suggested that MA crosslinked HFs were able to overcome the problem of poor matrix integrity and rapid erosion post-equilibrium, as observed in CA crosslinked HFs. However, the swellability of the hydrogel films decreased, which led to poor drug loading. This issue can be resolved by combining CMTG with other hydrophilic polymers having reactive hydroxyl groups or by using a combination of CA and MA as crosslinking agents for the preparation of CMTG HFs.

Authors contributions

Vishwajeet Ghorpade: Validation. Writing review and editing, Data curation

Remeth Dias: Visualization, Formal analysis.

Akanksha Gade: Methodology, Writing original draft

Sanjay Salgar: Methodology, Resources

Sanjay Banerjee: Supervision, Resources

Kailas Mali: Project administration. Investigation, Data curation, Conceptualization.

Acknowledgements

Authors are thankful to the Adv. Vaibhav (Dada) Patil, President of Loknete Hon. Hanmantrao Patil Charitable Trust, Vita for providing necessary facilities for carrying out the research work. Shivaji University, Kolhapur and NMR facility centre of Indian Institute of Science, Bangalore is acknowledged for assistance with analytical work. Also, authors are thankful to Chroma Laboratories, Telangana (India) for providing gift sample of moxifloxacin hydrochloride.

Competing interests

The authors declare that have no competing financial interests or personal relationships that could have appeared to influence the work reported.

Ethical approval

This article does not contain any studies with human participants performed by any of the authors. Further, article does not contains any animal studies.

Artificial intelligence (AI) use declaration

The authors declare that artificial intelligence-assisted tools were used solely for language editing and grammatical refinement of the manuscript. No AI tools were used for data generation, data analysis, statistical interpretation, figure creation, or result manipulation. All scientific content, experimental design, data analysis, interpretation, and conclusions are the sole responsibility of the authors.

Funding

This research received no specific grant from any funding agency in the public, commercial, or not-for-profit sectors.

References

1. Salunkhe NH, Mali KK, Sidwadkar PH, Pareek KM, Aundhakar AS. Synthesis and

characterization of citric acid crosslinked garden cress seeds mucilage hydrogel for controlled drug release. *J Drug Deliv Sci Technol* 2025;112:107270. doi: 10.1016/j.jddst.2025.107270

2. Hoare TR, Kohane DS. Hydrogels in drug delivery: Progress and challenges. *Polymer (Guildf)* 2008;49(8):1993-2007. doi: 10.1016/j.polymer.2008.01.027
3. Zarzycki R, Modrzejewska Z, Nawrotek K, Lek U. Drug Release From Hydrogel Matrices. *Ecol Chem Eng S* 2010;17(2):117-36.
4. Peppas NA. Hydrogels and drug delivery. *Curr Opin Colloid Interface Sci* 1997;2(5):531-7. doi: 10.1016/S1359-0294(97)80103-3
5. Ribeiro M, Simões M, Vitorino C, Mascarenhas-Melo F. Hydrogels in Cutaneous Wound Healing: Insights into Characterization, Properties, Formulation and Therapeutic Potential. *Gels* 2024;10(3):188. doi: 10.3390/gels10030188
6. Angaria N, Saini S, Hussain MS, Sharma S, Singh G, Khurana N, et al. Natural polymer-based hydrogels: versatile biomaterials for biomedical applications. *Int J Polym Mater Polym Biomater* 2024;73(17):1550-68. doi: 10.1080/00914037.2023.2301645
7. Alavarse AC, Frachini ECG, da Silva RLCG, Lima VH, Shavandi A, Petri DFS. Crosslinkers for polysaccharides and proteins: Synthesis conditions, mechanisms, and crosslinking efficiency, a review. *Int J Biol Macromol* 2022;202:558-96. doi: 10.1016/j.ijbiomac.2022.01.029
8. Muir VG, Burdick JA. Chemically Modified Biopolymers for the Formation of Biomedical Hydrogels. *Chem Rev* 2021;121(18):10908-49. doi: 10.1021/acs.chemrev.0c00923
9. Vasile C, Pamfil D, Stoleru E, Baican M. New Developments in Medical Applications of Hybrid Hydrogels Containing Natural Polymers. *Molecules* 2020;25(7):1539. doi: 10.3390/molecules25071539
10. Lu L, Yuan S, Wang J, Shen Y, Deng S, Xie L, et al. The Formation Mechanism of Hydrogels. *Curr Stem Cell Res Ther* 2018;13(7):490-6. doi: 10.2174/1574888X12666170612102706
11. Bao Z, Xian C, Yuan Q, Liu G, Wu J. Natural Polymer-Based Hydrogels with Enhanced Mechanical Performances: Preparation, Structure, and Property. *Adv Healthc Mater* 2019;8(17). doi: 10.1002/adhm.201900670
12. Nasution H, Harahap H, Dalimunthe NF, Ginting MHS, Jaafar M, Tan OOH, et al. Hydrogel and Effects of Crosslinking Agent on Cellulose-Based Hydrogels: A Review.

Gels 2022;8(9):568. doi: 10.3390/gels8090568

13. Dimida S, Barca A, Cancelli N, De Benedictis V, Raucci MG, Demitri C. Effects of Genipin Concentration on Cross-Linked Chitosan Scaffolds for Bone Tissue Engineering: Structural Characterization and Evidence of Biocompatibility Features. *Int J Polym Sci* 2017;2017:1-8. doi: 10.1155/2017/8410750
14. Garcia J, Hsieh MF, Doma B, Peruelo D, Chen IH, Lee HM. Synthesis of Gelatin-γ-Polyglutamic Acid-Based Hydrogel for the In Vitro Controlled Release of Epigallocatechin Gallate (EGCG) from Camellia sinensis. *Polymers (Basel)* 2013;6(1):39-58. doi: 10.3390/polym6010039
15. Iftime MM, Rosca I, Sandu AI, Marin L. Chitosan crosslinking with a vanillin isomer toward self-healing hydrogels with antifungal activity. *Int J Biol Macromol* 2022;205:574-86. doi: 10.1016/j.ijbiomac.2022.02.077
16. Liu WC, Wang HY, Lee TH, Chung RJ. Gamma-poly glutamate/gelatin composite hydrogels crosslinked by proanthocyanidins for wound healing. *Mater Sci Eng C* 2019;101:630-9. doi: 10.1016/j.msec.2019.04.018
17. Seidel C, Kulicke WM, Heb C, Hartmann B, Lechner MD, Lazik W. Influence of the Cross-linking Agent on the Gel Structure of Starch Derivatives. *Starch - Stärke* 2001;53(7):305-10. doi: 10.1002/1521-379X(200107)53:7<305::AID-STAR305>3.0.CO;2-Z
18. Sethi S, Medha, Singh G, Sharma R, Kaith BS, Sharma N, et al. Fluorescent hydrogel of chitosan and gelatin cross-linked with maleic acid for optical detection of heavy metals. *J Appl Polym Sci* 2022;139(15). doi: 10.1002/app.51941
19. Xu J, Boddu VM, Liu SX. Rheological properties of hydrogels produced by cellulose derivatives crosslinked with citric acid, succinic acid and sebacic acid. *Cellul Chem Technol* 2022;56(1-2):49-54. doi: 10.35812/CelluloseChemTechnol.2022.56.04
20. Mali K, Dhawale S, Dias R, Ghorpade V. Delivery of drugs using tamarind gum and modified tamarind gum: a review. *Bull Fac Pharm, Cairo Univ* 2019;57(1):1-24. doi: 10.21608/BFPC.2019.47260
21. Jana S, Sharma R, Maiti S, Sen KK. Interpenetrating hydrogels of O-carboxymethyl Tamarind gum and alginate for monitoring delivery of acyclovir. *Int J Biol Macromol* 2016;92:1034-9. doi: 10.1016/j.ijbiomac.2016.08.017
22. Shaw GS, Uvanesh K, Gautham SN, Singh V, Pramanik K, Kumar N, et al. Development and characterization of gelatin-tamarind gum / carboxymethyl tamarind gum based

phase- separated hydrogels : a comparative study. *Des Monomers Polym* 2015;18(5):434-50. doi: 10.1080/15685551.2015.1041075

23. Malik R, Warkar SG, Saxena R. Carboxy-methyl tamarind kernel gum based bio-hydrogel for sustainable agronomy. *Mater Today Commun* 2023;35:105473. doi: 10.1016/j.mtcomm.2023.105473
24. Meena P, Singh P, Warkar SG. Development and assessment of carboxymethyl tamarind kernel gum-based pH-responsive hydrogel for release of diclofenac sodium. *Eur Polym J* 2023;197:112340. doi: 10.1016/j.eurpolymj.2023.112340
25. Yadav P, Warkar SG, Kumar A. Development of graphene oxide-incorporated biopolymer-carboxymethyl tamarind kernel gum-based hydrogel as an effective adsorbent for the sequestration of dye pollutants. *Polym Eng Sci* 2024;64(10):4816-33. doi: 10.1002/pen.26883
26. Mali KK, Dhawale SC, Dias RJ. Synthesis and characterization of hydrogel films of carboxymethyl tamarind gum using citric acid. *Int J Biol Macromol* 2017;105(Pt 1):463-70. doi: 10.1016/j.ijbiomac.2017.07.058
27. Dudeja I, Mankoo RK, Singh A, Kaur J. Citric acid: An ecofriendly cross-linker for the production of functional biopolymeric materials. *Sustain Chem Pharm* 2023;36:101307. doi: 10.1016/j.scp.2023.101307
28. Shen L, Xu H, Kong L, Yang Y. Non-Toxic Crosslinking of Starch Using Polycarboxylic Acids: Kinetic Study and Quantitative Correlation of Mechanical Properties and Crosslinking Degrees. *J Polym Environ* 2015;23(4):588-94. doi: 10.1007/s10924-015-0738-3
29. Dolbow J, Fried E, Ji H. A numerical strategy for investigating the kinetic response of stimulus-responsive hydrogels. *Comput Methods Appl Mech Eng* 2005;194(42-44):4447-80. doi: 10.1016/j.cma.2004.12.004
30. Sharma L, Sharma HK, Saini CS. Edible films developed from carboxylic acid cross-linked sesame protein isolate: barrier, mechanical, thermal, crystalline and morphological properties. *J Food Sci Technol* 2018;55(2):532-9. doi: 10.1007/s13197-017-2962-4
31. Bisla V, Yoshitake H. Control of mechanical and hydrophobic properties of silylated chitosan-starch films by cross-linking using carboxylic acids. *Carbohydr Polym Technol Appl* 2024;7(February):100462. doi: 10.1016/j.carpta.2024.100462
32. Priya G, Narendrakumar U, Manjubala I. Thermal behavior of carboxymethyl cellulose

in the presence of polycarboxylic acid crosslinkers. *J Therm Anal Calorim* 2019;138(1):89-95. doi: 10.1007/s10973-019-08171-2

33. Teramoto N, Ozeki M, Fujiwara I, Shibata M. Crosslinking and biodegradation of poly(butylene succinate) prepolymers containing itaconic or maleic acid units in the main chain. *J Appl Polym Sci* 2005;95(6):1473-80. doi: 10.1002/app.21393
34. Gautam L, Warkar SG, Jain M. Physicochemical evaluation of polyvinyl alcohol films crosslinked with saturated and unsaturated dicarboxylic acids: A comparative study. *Polym Eng Sci* 2024;64(8):3703-15. doi: 10.1002/pen.26806
35. El-sheikh MA. A novel photo-grafting of acrylamide onto carboxymethyl starch. 1. Utilization of CMS-g-PAAm in easy care finishing of cotton fabrics. *Carbohydr Polym* 2016;152:105-18. doi: 10.1016/j.carbpol.2016.06.088
36. Salam A, Pawlak JJ, Venditti R a., El-tahlawy K. Incorporation of carboxyl groups into xylan for improved absorbency. *Cellulose* 2011;18(4):1033-41. doi: 10.1007/s10570-011-9542-y
37. Ghorpade VS, Yadav AV, Dias RJ. Citric acid crosslinked β -cyclodextrin/carboxymethylcellulose hydrogel films for controlled delivery of poorly soluble drugs. *Carbohydr Polym* 2017;164:339-48. doi: 10.1016/j.carbpol.2017.02.005
38. Hussain R, Minhas B, Batool SA, Kazmi SL, Javed U, Abbas Z, et al. Electrophoretically deposited Asphaltum punjabianum (Shilajit) coatings on polyvinylalcohol/carboxymethylcellulose hydrogels. *Int J Biol Macromol* 2024;278:134699. doi: 10.1016/j.ijbiomac.2024.134699
39. Avachat AM, Gujar KN, Wagh K V. Development and evaluation of tamarind seed xyloglucan-based mucoadhesive buccal films of rizatriptan benzoate. *Carbohydr Polym* 2013;91(2):537-42. doi: 10.1016/j.carbpol.2012.08.062
40. Zhang F, Han X, Guo C, Yang H, Wang J, Wu X. Fibrous aramid hydrogel supported antibacterial agents for accelerating bacterial-infected wound healing. *Mater Sci Eng C* 2021;121:111833. doi: 10.1016/j.msec.2020.111833
41. Lowery OH, Rosebrough NJ, Lewis Farr A, Randall RJ. Protein measurement with the folin phenol reagent. *J Biol Chem* 1951;193:265-75.
42. Singh B, Dhiman A. Designing bio-mimetic moxifloxacin loaded hydrogel wound dressing to improve antioxidant and pharmacology properties. *RSC Adv* 2015;5(55):44666-78. doi: 10.1039/C5RA06857F

43. Chambi HNM, Grosso CRF. Mechanical and water vapor permeability properties of biodegradables films based on methylcellulose, glucomannan, pectin and gelatin. *Ciência e Tecnol Aliment* 2011;31(3):739-46. doi: 10.1590/S0101-20612011000300029
44. Wittayaareekul S, Prahsarn C. Development and in vitro evaluation of chitosan–polysaccharides composite wound dressings. *Int J Pharm* 2006;313(1-2):123-8. doi: 10.1016/j.ijpharm.2006.01.027
45. Chen J, Park K. Synthesis and characterization of superporous hydrogel composites. *J Control Release* 2000;65(1-2):73-82. doi: 10.1016/S0168-3659(99)00238-2
46. Singh B, Sharma S, Dhiman A. Design of antibiotic containing hydrogel wound dressings: Biomedical properties and histological study of wound healing. *Int J Pharm* 2013;457(1):82-91. doi: 10.1016/j.ijpharm.2013.09.028
47. Chalitangkoon J, Wongkittisin M, Monvisade P. Silver loaded hydroxyethylacryl chitosan/sodium alginate hydrogel films for controlled drug release wound dressings. *Int J Biol Macromol* 2020;159:194-203. doi: 10.1016/j.ijbiomac.2020.05.061
48. Ghosal K, Das A, Das SK, Mahmood S, Ramadan MAM, Thomas S. Synthesis and characterization of interpenetrating polymeric networks based bio-composite alginate film: A well-designed drug delivery platform. *Int J Biol Macromol* 2019;130:645-54. doi: 10.1016/j.ijbiomac.2019.02.117
49. Ritger PL, Peppas NA. A simple equation for description of solute release II. Fickian and anomalous release from swellable devices. *J Control Release* 1987;5(1):37-42. doi: 10.1016/0168-3659(87)90035-6
50. Demitri C, Del Sole R, Scalera F, Sannino A, Vasapollo G, Maffezzoli A, et al. Novel superabsorbent cellulose-based hydrogels crosslinked with citric acid. *J Appl Polym Sci* 2008;110(4):2453-60. doi: 10.1002/app.28660
51. Kumar R, Park K, Ahn K, Ansari JR, Sadeghi K, Seo J. Maleic acid crosslinked starch/polyvinyl alcohol blend films with improved barrier properties for packaging applications. *Int J Biol Macromol* 2024;271:132495. doi: 10.1016/j.ijbiomac.2024.132495
52. Abou-Yousef H, Kamel S. High efficiency antimicrobial cellulose-based nanocomposite hydrogels. *J Appl Polym Sci* 2015;132(31):1-9. doi: 10.1002/app.42327
53. Khadsai S, Janmanee R, Sam-Ang P, Nuanchawee Y, Rakitikul W, Mankhong W, et al. Influence of Crosslinking Concentration on the Properties of Biodegradable Modified

Cassava Starch-Based Films for Packaging Applications. *Polymers (Basel)* 2024;16(12):1647. doi: 10.3390/polym16121647

54. Apelblat A, Manzurola E. Solubility of oxalic, malonic, succinic, adipic, maleic, malic, citric, and tartaric acids in water from 278.15 to 338.15 K. *J Chem Thermodyn* 1987;19(3):317-20. doi: 10.1016/0021-9614(87)90139-X
55. Erceg T, Stupar A, Cvetinov M, Vasić V, Ristić I. Investigation the correlation between chemical structure and swelling, thermal and flocculation properties of carboxymethylcellulose hydrogels. *J Appl Polym Sci* 2021;138(10):1-16. doi: 10.1002/app.50240
56. Shafiq K, Mahmood A, Salem-Bekhit MM, Sarfraz RM, Algarni AS, Taha EI, et al. Development and Optimization of Tamarind Gum-β-Cyclodextrin-g-Poly(Methacrylate) pH-Responsive Hydrogels for Sustained Delivery of Acyclovir. *Pharmaceuticals* 2022;15(12):1527. doi: 10.3390/ph15121527
57. Khushbu, Warkar SG, Thombare N. Zinc micronutrient-loaded carboxymethyl tamarind kernel gum-based superabsorbent hydrogels: controlled release and kinetics studies for agricultural applications. *Colloid Polym Sci* 2021;299(7):1103-11. doi: 10.1007/s00396-021-04831-8
58. Vogler EA. Structure and reactivity of water at biomaterial surfaces. *Adv Colloid Interface Sci* 1998;74(1-3):69-117. doi: 10.1016/S0001-8686(97)00040-7
59. Kuddushi M, Deng X, Nayak J, Zhu S, Xu B Bin, Zhang X. A Transparent, Tough and Self-Healable Biopolymeric Composites Hydrogel for Open Wound Management. *ACS Appl Bio Mater* 2023;6(9):3810-22. doi: 10.1021/acsabm.3c00455
60. Qiu X, Zhang J, Cao L, Jiao Q, Zhou J, Yang L, et al. Antifouling Antioxidant Zwitterionic Dextran Hydrogels as Wound Dressing Materials with Excellent Healing Activities. *ACS Appl Mater Interfaces* 2021;13(6):7060-9. doi: 10.1021/acsami.0c17744
61. Lalani R, Liu L. Electrospun Zwitterionic Poly(Sulfobetaine Methacrylate) for Nonadherent, Superabsorbent, and Antimicrobial Wound Dressing Applications. *Biomacromolecules* 2012;13(6):1853-63. doi: 10.1021/bm300345e
62. Lachenbruch C, VanGilder C. Estimates of Evaporation Rates from Wounds for Various Dressing/Support Surface Combinations. *Adv Skin Wound Care* 2012;25(1):29-36. doi: 10.1097/01.ASW.0000410688.21987.1d
63. Lan Z, Kar R, Chwatko M, Shoga E, Cosgriff-Hernandez E. High porosity PEG-based

hydrogel foams with self-tuning moisture balance as chronic wound dressings. *J Biomed Mater Res Part A* 2023;111(4):465-77. doi: 10.1002/jbm.a.37498

64. Yang S, Lan L, Gong M, Yang K, Li X. An asymmetric wettable PCL/chitosan composite scaffold loaded with IGF-2 for wound dressing. *J Biomater Appl* 2022;37(4):577-87. doi: 10.1177/08853282221110315
65. Augustine R, Hasan A, Patan NK, Augustine A, Dalvi YB, Varghese R, et al. Titanium Nanorods Loaded PCL Meshes with Enhanced Blood Vessel Formation and Cell Migration for Wound Dressing Applications. *Macromol Biosci* 2019;19(7):e1900058. doi: 10.1002/mabi.201900058
66. Gao W, Jin W, Li Y, Wan L, Wang C, Lin C, et al. A highly bioactive bone extracellular matrix-biomimetic nanofibrous system with rapid angiogenesis promotes diabetic wound healing. *J Mater Chem B* 2017;5(35):7285-96. doi: 10.1039/C7TB01484H
67. Loveday HP, Wilson JA, Pratt RJ, Golsorkhi M, Tingle A, Bak A, et al. epic3: National Evidence-Based Guidelines for Preventing Healthcare-Associated Infections in NHS Hospitals in England. *J Hosp Infect* 2014;86:S1-70. doi: 10.1016/S0195-6701(13)60012-2
68. Kunimitsu M, Nakagami G, Kitamura A, Minematsu T, Koudounas S, Ogai K, et al. Relationship between healing status and microbial dissimilarity in wound and peri-wound skin in pressure injuries. *J Tissue Viability* 2023;32(1):144-50. doi: 10.1016/j.jtv.2022.10.006
69. Mertz PM, Ovington LG. Wound Healing Microbiology. *Dermatol Clin* 1993;11(4):739-47. doi: 10.1016/S0733-8635(18)30226-2
70. Khan S, Ranjha NM. Effect of degree of cross-linking on swelling and on drug release of low viscous chitosan/poly(vinyl alcohol) hydrogels. *Polym Bull* 2014;71(8):2133-58. doi: 10.1007/s00289-014-1178-2
71. Mahkam M, Doostie L. The Relation Between Swelling Properties and Cross-Linking of Hydrogels Designed for Colon-Specific Drug Delivery. *Drug Deliv* 2005;12(6):343-7. doi: 10.1080/10717540590952627
72. Agarwal T, Narayana SN, Pal K, Pramanik K, Giri S, Banerjee I. Calcium alginate-carboxymethyl cellulose beads for colon-targeted drug delivery. *Int J Biol Macromol* 2015;75:409-17. doi: 10.1016/j.ijbiomac.2014.12.052
73. Gu R, Zhou H, Zhang Z, Lv Y, Pan Y, Li Q, et al. Research progress related to

thermosensitive hydrogel dressings in wound healing: a review. *Nanoscale Adv* 2023;5(22):6017-37. doi: 10.1039/D3NA00407D

74. Ghorpade VS, Yadav AV, Dias RJ, Mali KK, Pargaonkar SS, Shinde PV, et al. Citric acid crosslinked carboxymethylcellulose-poly(ethylene glycol) hydrogel films for delivery of poorly soluble drugs. *Int J Biol Macromol* 2018;118:783-91. doi: 10.1016/j.ijbiomac.2018.06.142
75. Ghorpade VS, Dias RJ, Mali KK, Mulla SI. Citric acid crosslinked carboxymethylcellulose-polyvinyl alcohol hydrogel films for extended release of water soluble basic drugs. *J Drug Deliv Sci Technol* 2019;52:421-30. doi: 10.1016/j.jddst.2019.05.013
76. Mali KK, Ghorpade VS, Dias RJ, Dhawale SC. Synthesis and characterization of citric acid crosslinked carboxymethyl tamarind gum-polyvinyl alcohol hydrogel films. *Int J Biol Macromol* 2023;236:123969. doi: 10.1016/j.ijbiomac.2023.123969
77. Fenyvesi E, Vikmon M, Szeman J, Redenti E, Delcanale M, Ventura P, et al. Interaction of Hydroxy Acids with β-Cyclodextrin. *J Incl Phenom Macrocycl Chem* 1999;33(3):339-44. doi: 10.1023/A:1008094702632
78. Uyanga KA, Okpozo OP, Onyekwere OS, Daoud WA. Citric acid crosslinked natural bi-polymer-based composite hydrogels: Effect of polymer ratio and beta-cyclodextrin on hydrogel microstructure. *React Funct Polym* 2020;154:104682. doi: 10.1016/j.reactfunctpolym.2020.104682
79. Rumon MMH, Rahman MS, Akib AA, Sohag MS, Rakib MRA, Khan MAR, et al. Progress in hydrogel toughening: addressing structural and crosslinking challenges for biomedical applications. *Discov Mater* 2025;5(1):5. doi: 10.1007/s43939-025-00178-x
80. Guay DR. Moxifloxacin in the treatment of skin and skin structure infections. *Ther Clin Risk Manag* 2006;2(4):417-34. doi: 10.2147/tcrm.2006.2.4.417
81. Efe H, Bicen M, Kahraman MV, Kayaman-Apohan N. Synthesis of 4-Acryloylmorpholine-based Hydrogels and Investigation of their Drug Release Behaviors. *J Braz Chem Soc* 2013;24(5):814-20. doi: 10.5935/0103-5053.20130107
82. Choy Y Bin, Cheng F, Choi H, Kim K (Kevin). Monodisperse Gelatin Microspheres as a Drug Delivery Vehicle: Release Profile and Effect of Crosslinking Density. *Macromol Biosci* 2008;8(8):758-65. doi: 10.1002/mabi.200700316
83. Pouroutzidou GK, Liverani L, Theocharidou A, Tsamesidis I, Lazaridou M, Christodoulou E, et al. Synthesis and Characterization of Mesoporous Mg- and Sr-Doped Nanoparticles

for Moxifloxacin Drug Delivery in Promising Tissue Engineering Applications. *Int J Mol Sci* 2021;22(2):577. doi: 10.3390/ijms22020577

84. Abka-khajouei R, Tounsi L, Shahabi N, Patel AK, Abdelkafi S, Michaud P. Structures, Properties and Applications of Alginates. *Mar Drugs* 2022;20(6):364. doi: 10.3390/md20060364

85. Bazban-Shotorbani S, Hasani-Sadrabadi MM, Karkhaneh A, Serpooshan V, Jacob KI, Moshaverinia A, et al. Revisiting structure-property relationship of pH-responsive polymers for drug delivery applications. *J Control Release* 2017;253:46-63. doi: 10.1016/j.jconrel.2017.02.021

86. Tonannavar J, Chavan YB, Yenagi J. (R)-(−)-2-Pyrrolidinemethanol: A combined experimental and DFT vibrational analysis of monomers, dimers and hydrogen bonding. *Spectrochim Acta Part A Mol Biomol Spectrosc* 2015;149:860-8. doi: 10.1016/j.saa.2015.04.020

87. Dimitrova Y. Theoretical study of the changes in the vibrational characteristics arising from the hydrogen bonding between Vitamin C (l-ascorbic acid) and H2O. *Spectrochim Acta Part A Mol Biomol Spectrosc* 2006;63(2):427-37. doi: 10.1016/j.saa.2005.03.037

88. Xiong X, He J, Yang H, Tang P, Tang B, Sun Q, et al. Investigation on the interaction of antibacterial drug moxifloxacin hydrochloride with human serum albumin using multi-spectroscopic approaches, molecular docking and dynamical simulation. *RSC Adv* 2017;7(77):48942-51. doi: 10.1039/C7RA08731D

89. Al Omari MMH, Jaafari DS, Al-Sou'od KA, Badwan AA. Moxifloxacin Hydrochloride. In: *Profiles of Drug Substances, Excipients, and Related Methodology*. Vol 39. Burlington: Academic Press; 2014. P. 299-431. doi: 10.1016/B978-0-12-800173-8.00007-6

90. Kulkarni C V., Moinuddin Z, Patil-Sen Y, Littlefield R, Hood M. Lipid-hydrogel films for sustained drug release. *Int J Pharm* 2015;479(2):416-21. doi: 10.1016/j.ijpharm.2015.01.013

91. Fanse S, Bao Q, Zou Y, Wang Y, Burgess DJ. Impact of polymer crosslinking on release mechanisms from long-acting levonorgestrel intrauterine systems. *Int J Pharm* 2022;612:121383. doi: 10.1016/j.ijpharm.2021.121383

92. Mauri E, Chincarini GMF, Rigamonti R, Magagnin L, Sacchetti A, Rossi F. Modulation of electrostatic interactions to improve controlled drug delivery from nanogels. *Mater Sci Eng C* 2017;72:308-15. doi: 10.1016/j.msec.2016.11.081

93. Makino K, Idenuma R, Murakami T, Ohshima H. Design of a rate- and time-programming drug release device using a hydrogel: pulsatile drug release from κ-carrageenan hydrogel device by surface erosion of the hydrogel. *Colloids Surfaces B Biointerfaces* 2001;20(4):355-9. doi: 10.1016/S0927-7765(00)00207-1

94. Chopra L, Thakur KK, Chohan JS, Sharma S, Ilyas RA, Asyraf MRM, et al. Comparative Drug Release Investigations for Diclofenac Sodium Drug (DS) by Chitosan-Based Grafted and Crosslinked Copolymers. *Materials (Basel)* 2022;15(7):2404. doi: 10.3390/ma15072404

95. Feyissa Z, Edossa GD, Bedasa TB, Inki LG. Fabrication of pH-Responsive Chitosan/Polyvinylpyrrolidone Hydrogels for Controlled Release of Metronidazole and Antibacterial Properties. Wu Q, editor. *Int J Polym Sci* 2023;2023:1-18. doi: 10.1155/2023/1205092

96. Akakuru O, Isiuku B. Chitosan Hydrogels and their Glutaraldehyde-Crosslinked Counterparts as Potential Drug Release and Tissue Engineering Systems - Synthesis, Characterization, Swelling Kinetics and Mechanism. *J Phys Chem Biophys* 2017;07(03):1-7. doi: 10.4172/2161-0398.1000256

97. García-Couce J, Vernhes M, Bada N, Agüero L, Valdés O, Alvarez-Barreto J, et al. Synthesis and Evaluation of AlgNa-g-Poly(QCL-co-HEMA) Hydrogels as Platform for Chondrocyte Proliferation and Controlled Release of Betamethasone. *Int J Mol Sci* 2021;22(11):5730. doi: 10.3390/ijms22115730

98. Mountaki SA, Kaliva M, Loukelis K, Chatzinikolaidou M, Vamvakaki M. Responsive Polyesters with Alkene and Carboxylic Acid Side-Groups for Tissue Engineering Applications. *Polymers (Basel)* 2021;13(10):1636. doi: 10.3390/polym13101636

99. do Nascimento FC, de Aguiar LCV, Costa LAT, Fernandes MT, Marassi RJ, Gomes A de S, et al. Formulation and characterization of crosslinked polyvinyl alcohol (PVA) membranes: effects of the crosslinking agents. *Polym Bull* 2021;78(2):917-29. doi: 10.1007/s00289-020-03142-2